

Numerical Analysis of the Dynamic Response of a Single-Point Mooring Fish Cage in Waves and Currents

Xiaohua Huang^{1, 2, *} , Haiyang Liu², Qiyu Tao³, Yu Hu³, Shaomin Wang³, Taiping Yuan³

¹ Key Lab. of Open-Sea Fishery Development, Ministry of Agriculture, Guangzhou 510300, China.

² Tropical Fisheries Research and Development Center, South China Sea Fisheries Research Institute, Chinese Academy of Fishery Sciences, Sanya 572018, China.

³ South China Sea Fisheries Research Institute, Guangdong Cage Engineering Research Center, Guangzhou 510300, China.

Article History

Received 14 January 2019

Accepted 29 March 2019

First Online 02 April 2019

Corresponding Author

Tel.: +862034066940

E-mail: huangx-hua@163.com

Keywords

Dynamic response

Finite element model

Fish cage

Floating collar deformation

Single point mooring

Abstract

In this study, we developed a numerical model of a single-point mooring (SPM) cage system based on the finite element method, and employed it to simulate the dynamic response of the cage system under conditions with waves and currents. We focused mainly on the mooring line tension and deformation for the cage collar. The simulated results indicated that adding a buoy as part of a cage system was helpful for reducing the force and deformation of the cage collar, and the current contributed greatly to the total load on the cage system. In addition, the location of the greatest deformation of the cage collar was confirmed by comparing the stress results for different points in the collar structure when exposed to strong waves and current. Therefore, to avoid plastic failure, we tested a connected component with a lower pipe diameter to wall thickness ratio to effectively reduce the deformation of the floating pipes, thereby enhancing the security of the SPM cage system under severe sea conditions. Furthermore, we analyzed and discussed the effects of the material characteristics on the dynamic properties of the SPM cage system.

Introduction

Capture fishery production has remained relatively static since the late 1980s, and thus the utilization of aquaculture has increased to supply fish for human consumption. Aquaculture production has increased the total seafood consumed throughout the world by up to 40% (FAO, 2016). However, due to various environmental issues and coastal zone resource conflicts in recent years, fish farming has tended to shift to more exposed locations. Moving fish farms to areas with strong waves and currents can improve production by providing more stable temperatures and improving the water quality, as well as reducing the environmental impacts of modern fish farming (Klebert *et al.*, 2015). In

China, net cages are used widely in offshore fish farming and these cages tend to have larger dimensions. Considering the severe conditions in the sea, then to obtain the benefits of cage farming in open areas, the cage system employed needs to have excellent structural strength to withstand the heavy loads due to strong winds, waves, and currents, thereby demanding the design of effective net cages and mooring systems.

In the offshore net cage systems, the types of moorings employed comprise the multiple point mooring system (MPM) and single point mooring system (SPM) (see Figure 1). In the MPM system, the relatively stable positions of the cage systems in offshore sea areas make cage culture management convenient and easy for the farmer, although the net cage is subjected

to waves and currents from different directions. However, due to the requirement for the precise and tight adjustment of multiple anchors (Goudey *et al.*, 2001), the marine installation of MPM systems becomes more difficult and the mooring costs are higher as the water depth increases. Compared with the MPM system, one of the advantages of the SPM system is the substantially reduced benthic accumulation of waste products because the fish waste is distributed over a larger area. Another advantage is a possible reduction in mooring costs, which can be halved or even lower (DeCew *et al.*, 2010). In addition, the cage system responds to the changes in waves and currents rather than resisting them, which helps to minimize the environmental loading on the mooring components.

Cage system designers, installers and fish farmers must consider how the performance of fish cages is influenced by severe sea loads. Therefore, numerous studies have been conducted to analyze the hydrodynamic behavior of net cage systems based on numerical simulation methods, physical model testing, or field measurements. Previous studies have investigated all of the cage components, including the cage collar, fishing net and mooring system. Huang *et al.* (2008) analyzed the effects of waves with a uniform current on the mooring line tension and net deformation for marine aquaculture gravity-type cages equipped with the MPM system by using a numerical model, which was validated with physical model tests. Kristiansen and Faltinsen (2012, 2015) proposed a screen type of force model for the viscous hydrodynamic load on nets and investigated the mooring loads on a net cage in currents and waves. DeCew *et al.* (2013) used an acoustic method to monitor the movement and deformation of a small-scale fish cage in currents, and they compared their results with field measurements. The floating collar is a critical component of fish cages because it is responsible for providing buoyancy to ensure cage drifting and to act as an operational platform for farm workers, but it also has a significant role in resisting impacts due to sea loads. However, hydrodynamic experimental tests of fish cages have that a small-scale cage collar is not likely to meet the stiffness similarity criterion because the cage collar basically behaves as a rigid body in a water tank (Ding *et al.*, 2007; Xu *et al.*, 2013), especially when focusing only on net deformation in a cage system under currents (Moe *et al.*, 2010; Lader and Enerhaug, 2005; Stranda, 2016). In practice, a cage collar made of high-density polyethylene (HDPE) may deform greatly when the net cage is impacted by heavy sea loads. Site observations have confirmed that the deformation of larger fish cages is more severe than smaller cages (Hao, 2008). Several studies have investigated the deformation of cage flotation structures using numerical models (Fredriksson *et al.*, 2007; Li *et al.*, 2013; Huang *et al.*, 2016; Xu *et al.*, 2017; Huang *et al.*, 2018), which is a practical and effective approach.

SPM cage systems are favorable for offshore fish farming because of their environmentally friendly and economically beneficial characteristics, and thus they have attracted the interest of researchers in the marine aquacultural community. For example, Shainee *et al.* (2013) investigated the submergence characteristics of an SPM cage system in regular waves with a following current. Xu *et al.* (2014) also analyzed the hydrodynamic behavior of a self-submersible SPM gravity cage in a combined wave-current flow, where they considered the effects on the submergence performance of the frontal rigid frame, the depth of the junction point, and the slope of the anchor line. However, if an SPM cage experiences severe weather, especially natural disasters such as typhoons, failure may occur due to plastic deformation of the cage collar as a consequence of the excessive mooring line tension and heavy sea loads. Therefore, reducing the mooring line tension and enhancing the bearing capacity of the collar structure are very important for decreasing the risk of failure and ensuring the successful operation of SPM cages in offshore waters.

In this study, we analyze the dynamic response of an SPM cage system (see Figure 1) when subjected to the action of waves and currents in order to optimize the design to increase the bearing capacity of an SPM cage. The remainder of this paper is organized as follows. In Section 2, we provide a description of the SPM cage system. In Section 3, we briefly introduce the finite element numerical model of a fish cage and we describe the calculation of various loads. We analyze the effects of the mooring arrangement, waves and currents, and material characteristics on the mooring line tension and cage collar deformation in Section 4. Finally, we give our conclusions.

Description of the SPM cage system

The SPM cage illustrated in Figure 2 was designed by South China Sea Fisheries Research Institute, CAFS. In this study, we aim to determine whether the SPM cage can be used efficiently in offshore conditions by analyzing its dynamic response. We do not provide a full explanation of the detailed design of the cage system, but instead the overall structure is described briefly as follows. The important parts of the cage system in the floating collar structure comprise the floating pipes, hand rail, and vertical supports. Overall, the floating pipes constitute three trapezoids connected by three pipes with a length of 7.6 m, which is the same as the length of the bottom edge of each trapezoid. The three pipes combine with the bottom edge of each trapezoid to form a regular hexagon, where the length of each side is 7.6 m. In addition, a vertical pipe is located at the middle portion of each trapezoid, which gives the structure stiffness. Any one corner of the overall collar structure, which is also identified as the upper portion of each trapezoid, can be used for providing a fixation at

Table 1. Geometric and material properties of the cage system

Component	Parameter	Value
Floating pipe	Pipe diameter	0.4 m
	Wall thickness	23.5 mm
	Material	HDPE
	Modulus of elasticity	950 MPa
	Poissons ratio	0.42
	Yield stress	24 MPa
Net	Mesh size	0.045 m
	Twine diameter	2 mm
	Height	6 m
	Material	PE
Mooring line	Solidity	4%
	Length	60 m
	Diameter	0.04 m
Buoy	Material	PE
	Axial stiffness	260 kN
	Height	2 m
	Diameter	1.5 m
Sinkers	Weight	30 kg
	Mass	20×20 kg
	Height	0.3 m
	Material	Concrete

Calculating the Loads on the Net Cage

The structural model of a line used to represent different parts of net cage is a massless element with a node at each end. All of the loads related to each line segment, such as the weight, buoyancy, hydrodynamic drag, added mass, tension and shear, and bending moment, are lumped and assigned to the node. The equation of motion (Newton's law) is then formulated for each line node as follows:

$$\mathbf{M}(\mathbf{p}, \mathbf{a}) = \mathbf{F}(\mathbf{p}, \mathbf{v}, t) - \mathbf{C}(\mathbf{p}, \mathbf{v}) - \mathbf{K}(\mathbf{p}) \quad (1)$$

where $\mathbf{M}(\mathbf{p}, \mathbf{a})$ is the system inertia load, $\mathbf{F}(\mathbf{p}, \mathbf{v}, t)$ is the external load, $\mathbf{C}(\mathbf{p}, \mathbf{v})$ is the system damping load, $\mathbf{K}(\mathbf{p})$ is the system stiffness load, t is the simulation time, and \mathbf{p} , \mathbf{v} , and \mathbf{a} are the position, velocity, and acceleration vectors, respectively. The local equation of motion is solved for the acceleration vector at the beginning of each time step for each line node, and then integrated using semi-implicit Euler integration (Orcina, 2015). At the end of each time step, the positions and orientations of all nodes are again known and the process is repeated.

The effective tension on each line segment when modeling different parts of the net cage structure can be expressed together using the following formula:

$$\mathbf{T}_e = \mathbf{T}_w + (\mathbf{P}_0 A_0 - \mathbf{P}_i A_i) \quad (2)$$

where \mathbf{T}_w represents the wall tension, which can be written as:

$$\mathbf{T}_w = EA\varepsilon - 2\mu(\mathbf{P}_0 A_0 - \mathbf{P}_i A_i) + EAC(dL/dt)/L_0 \quad (3)$$

where EA is the axial stiffness of the line, ε is the total mean axial strain given by $(L-L_0)/L_0$, L and L_0 are the instantaneous length and unstretched length of the segment, respectively, μ is Poisson ratio, \mathbf{P}_i and \mathbf{P}_0 are the internal and external (i.e., surrounding fluid) pressures, A_i and A_0 are the internal and external cross-sectional stress areas, C is a damping coefficient, and dL/dt is the rate of increase in the length. $\mathbf{P}_0 A_0$ is equal to $\mathbf{P}_i A_i$ for the fishing net and mooring lines of the net cage,

For the collar structure, the bending moment of each line segment is generated by the bending spring-damper for each node and its magnitude is:

$$|\mathbf{M}| = EI|\mathbf{k}| + (\lambda_b/100)D_c d|\mathbf{k}|/dt \quad (4)$$

where EI is the bending stiffness of a segment, \mathbf{k} is the curvature vector, λ_b is the target bending damping, and D_c is the bending critical damping value for a segment, which is given by $L_0(mEI/L_0)^{1/2}$. The node experiences two bending moments, \mathbf{M}_1 and \mathbf{M}_2 , i.e., one each from the segments on each of its sides.

The hydrodynamic loads over the net cage are calculated based on a modified version of the Morison equation by considering the relative motion between

the line element and fluid flow (Haritos and He, 1992). The two force components comprising the drag force and inertia force are described by Eq. (5). The drag forces applied to a line element are calculated using the cross-flow principle. Thus, the fluid velocity relative to the line V_r is split into its components that are normal and parallel to the line axis:

$$F_w = \frac{1}{2} \rho C_d S V_r |V_r| + \rho \nabla_w a_f + \rho \nabla_w C_a a_r \quad (5)$$

where F_w is the fluid force, ρ is the density of sea water, S is the drag area, V_r is the water particle velocity relative to the segment, ∇_w is the volume of water displaced by the segment, a_f is the water particle acceleration, a_r is the water particle acceleration relative to the segment, and C_d and C_a are the drag coefficient and added mass coefficient, respectively which are set to 1.2 and 1.0. In this formulation, V_r considers the superposition of the current and wave orbital velocities. When the current is steady, its contribution to water particle acceleration is zero.

Interaction with the Sea Surface

For a partially submerged line segment, the buoyancy is apportioned according to how much of the segment is submerged. For the floating collar under wave loads, the immersion depth of each line segment changes with the wave movements. We employ the concept of the proportion wet P_w (Figure 3) to calculate the buoyancy of each line segment in the collar structure, as follows:

$$F_B = P_w \rho g \nabla_B \quad (6)$$

where ∇_B is the line segment volume. We employ the diagonal line joining the highest point on the segment circumference at the “dry” end with the lowest point at the “wet” end (Figure 3). As the segment passes through the tangent position, the diagonal line switches corners but the proportion wet varies continuously. Thus, the intersection of the diagonal line with the surface continues to give the appropriate proportion

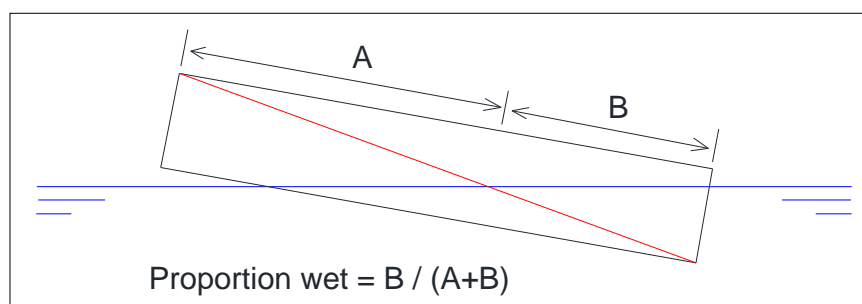


Figure 3. Proportion wet for a surface-piercing segment.

wet result. The ratio between the wet portion of the line and the total length of the line is defined as the proportion wet. The value of P_w is in the range 0 to 1, where a value of 0 denotes no submersion and 1 indicates completely submerged.

Pipe Stress Calculation

The cage collar made of HDPE is an elastic structure. Each position of the pipes in the collar structure may deform due to the effective tension, bending moment, and shear force as a consequence of the sea loads acting on the cage collar. The stress generated by these loads varies across the cross section of the pipe. To reflect the maximum deformation for each position along the circumference of the pipe, the von Mises strain ϵ_{vm} and stress σ_{vm} are given as follows.

$$\epsilon_{vm} = \sqrt{\epsilon_{zz}^2 + \epsilon_{cc}^2 - \epsilon_{zz} \epsilon_{cc}} \quad (7)$$

$$\sigma_{vm} = \sqrt{\frac{(\sigma_1 - \sigma_2)^2 + (\sigma_2 - \sigma_3)^2 + (\sigma_3 - \sigma_1)^2}{2}} \quad (8)$$

where ϵ_{zz} is the axial strain due to the direct tensile strain and bending strain, ϵ_{cc} is the hoop strain and σ_1 , σ_2 , and σ_3 are the principal stresses. The von Mises stress σ_{vm} is often used as a yield criterion. If torsion is not included, the maximum value of the von Mises stress occurs at either the inner or outer fiber of the pipe. If the bending stress contribution is dominant, then the maximum will occur at the outer fiber.

Results and Discussion

Effect of the Mooring Line Arrangement

Under severe sea conditions, the sea loads acting on the SPM cage system can be transmitted to the anchor via the connection with a mooring line. A larger mooring line tension inevitably leads to greater deformation of the cage collar, which can increase the risk of breakage. As a consequence, reducing the maximum mooring force by optimizing the mooring arrangement is very important for the successful

operation of the SPM cage under heavy sea weather conditions. We specify two types of mooring arrangement: a mooring line with a buoy (Figure 2) and a mooring line without a buoy, where the lines connect point O with point A. The two types of mooring arrangement have the same line length, i.e., 60 m.

The results calculated for the mooring line tension and von Mises stress at point A for the two mooring arrangement under pure waves, pure current, and waves combined with current are compared in Figures 4–6, respectively. The cage is subjected to waves (height = 5 m and period = 9 s) or a steady current (flow velocity = 1.0 m/s) running in the positive x-direction. Under any of the three sea conditions, the maximum value for the mooring line tension and pipe stress at point A is smaller for the cage system with a buoy than that without a buoy, which indicates that adding a buoy as a part of a cage system could reduce the force and deformation of the cage collar. In addition, the force will increase greatly when we consider a current and waves. The maximum mooring line tension for the cage with a buoy in waves with a current is almost 35 kN, which is three times more than that in pure waves, and this also applies to the maximum stress (Figure 4 and Figure 6). This is why a strong current causes the severe deformation of the fishing net, thereby contributing greatly to the total load on the cage system. Thus, the significant effect of a

current should be considered in the dynamic analysis of the SPM cage system to further understand its bearing capacity.

Deformation of the Floating Collar

Based on the forgoing analysis, we conduct numerical simulation of the mooring line with a buoy as the mooring system for the cage to determine the dynamic response of the SPM cage system under the impact of strong waves and a current. Regular wave conditions (height = 5, 6, or 7 m; period = 9 s) and current conditions (flow velocity = 0.6, 1.0, or 1.5 m/s) are used in the calculations. To investigate the collar deformation, we set some points as A–H (marked in Figure 2) to determine the locations with greatest deformation in the collar structure based on comparisons of the results calculated at different points on the floating pipes.

Figure 7 shows the results calculated for the force and deformation for the whole cage system under various currents, and wave and current conditions, where the position of the cage in motion occurs at the instant of the maximum mooring line tension and the top line denotes the water surface. We can see that the tension is slightly larger in the lower mooring line than the upper mooring line because the presence of the

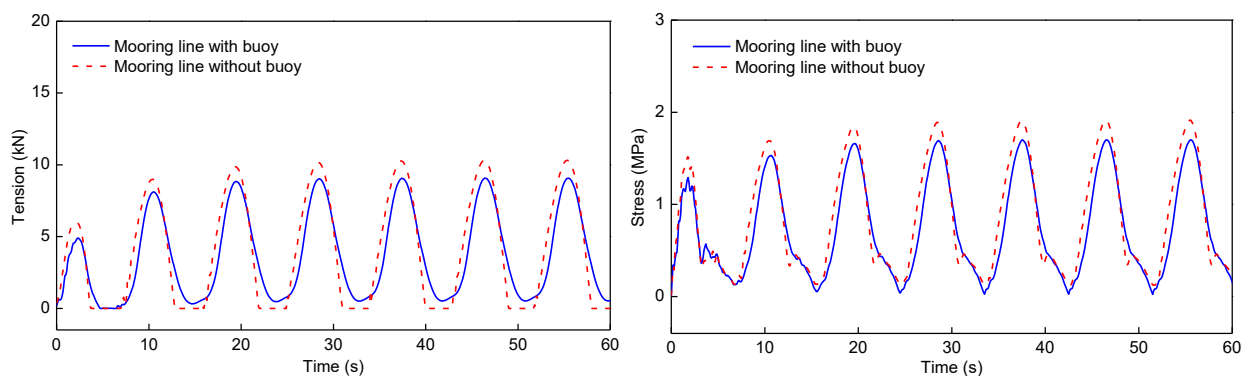


Figure 4. Mooring line tension and von Mises stress at point A under pure wave conditions with a height of 5 m and period of 9s.

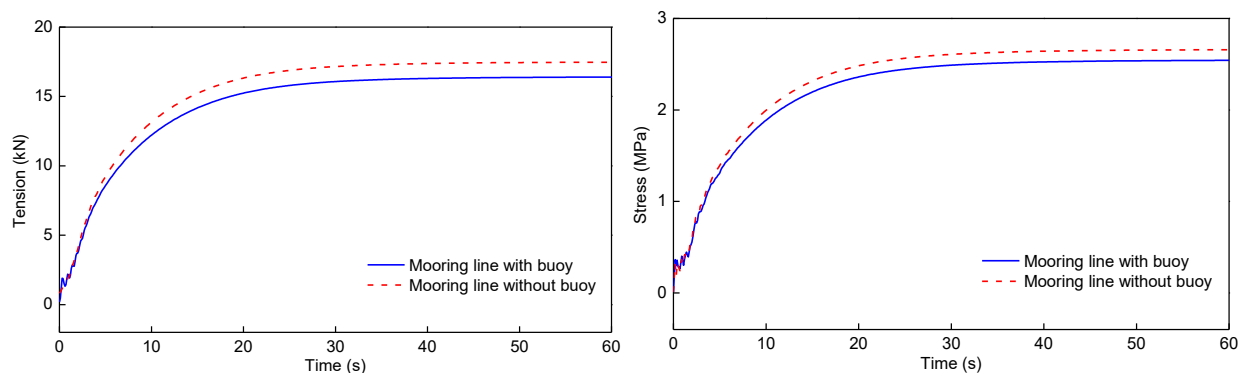


Figure 5. Mooring line tension and von Mises stress at point A under a current velocity of 1.0 m/s.

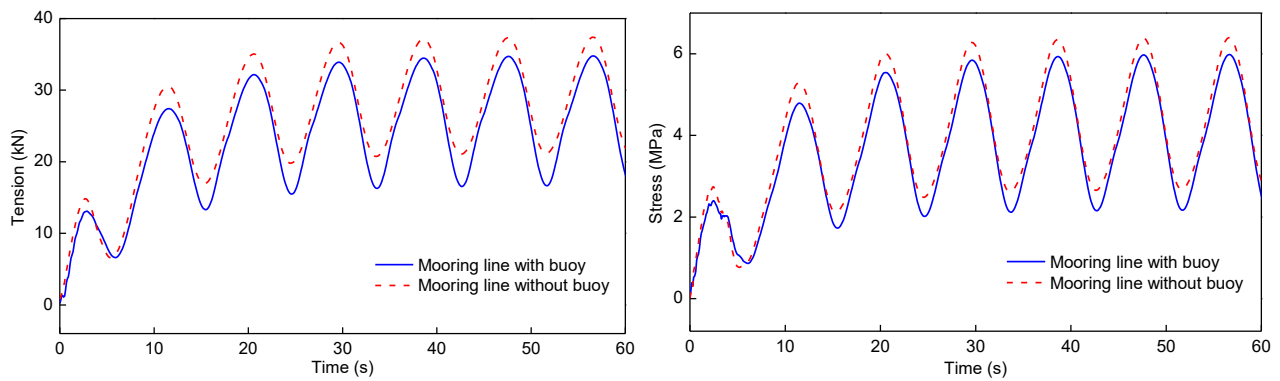


Figure 6. Mooring line tension and von Mises stress at point A under a wave height of 5 m, period of 9 s, and current velocity of 1.0 m/s.

buoy can help to reduce the tension in the upper mooring line. In the following, we use the maximum tension in the upper mooring line to represent the mooring line tension, unless stated otherwise. For the pure current conditions, the maximum tension increases rapidly when the current velocity becomes higher. The maximum tension is 32.05 kN at a flow velocity of 1.5 m/s, which is approximately four times more than that at a flow velocity of 0.6 m/s. A high speed current also leads to severe deformation of the fishing net. When the cage is subjected to sea loads with waves (height = 7 m and period = 9 s) and a current velocity of 1.5 m/s, the maximum tension is 77.64 kN, which is the largest among all of the different wave and current conditions (Figure 7). In this case, the mooring line is almost a straight line.

Table 2 lists the greatest pipe deformation results for different points on the floating collar under severe sea conditions with a wave height of 7 m and a current velocity of 1.5 m/s. The whole cage collar is symmetric on the X-axis, so we only consider eight points on the collar structure in the positive direction of the Y-axis. The deformation of point D is the highest among all of the different points attached to the floating pipes, followed by points C and A. In addition, the maximum von Mises stress is 22.79 MPa, which is very close to the yield stress of 24 MPa. Fredriksson *et al.* (2007) used the yield stress as a failure criterion to evaluate the plastic deformation of a floating pipe. Suitable measures to minimize the stress are very important for securing the collar structure to avoid plastic deformation at the connection position of point D. Thus, we propose the design of a component (Figure 8) as a connector placed at point D through fusion welding technology, where δ denotes the wall thickness of the pipe. The connector can also be placed at points C and G. SDR denotes the ratio of the pipe diameter relative to the wall thickness. The effects of SDR (17, 13.6, and 11) at a pipe diameter of 0.4 m for the connector on the bending moment and pipe stress at point D are shown in Figure 9. The maximum bending moment does not change

significantly for the connected component with different values of SDR. However, as shown in Figure 9, the maximum stress declines from 22.79 MPa to 16.94 MPa as SDR decreases for the connected component, which indicates the probability of plastic failure in the collar becomes lower.

Effects of Material Characteristics

The deformation and force for the SPM cage under the action of waves combined with a current may have strong relationships with the material characteristics, which are also important factors when considering for the security of fish cages. We consider various values of Young's modulus (from 600 to 1100 MPa) for the floating pipes and three levels of axial stiffness (260, 520, and 780 kN) for the mooring line to investigate their impacts on the dynamic properties of the SPM cage system. The wave-current conditions acting on the cage system are set as follows: wave height = 5 m, wave period = 9 s, and flow velocity = 1.0 m/s. Figure 10 illustrates the results calculated for the maximum mooring line tension and maximum strain for the cage collar with various values for Young's modulus. Clearly, the change in the tension on the mooring line is insignificant as Young's modulus increases, where the trend line for the tension is almost horizontal. However, under deformation of the collar structure, the strain decreases greatly from 1.82% to 1.08%. The effects of the axial stiffness of the mooring line on the force and deformation of the cage collar are shown in Figure 11, which indicates that the mooring line tension and strain tend to exhibit similar changes as the axial stiffness of the mooring line increases. The tension increases from 34.7 to 44.9 kN and the strain from 1.22% to 1.5% as EA varies up to 780 kN. This indicates that a mooring system with greater stiffness can cause higher deformation of the collar structure, which may increase the risk of failure for the cage system.

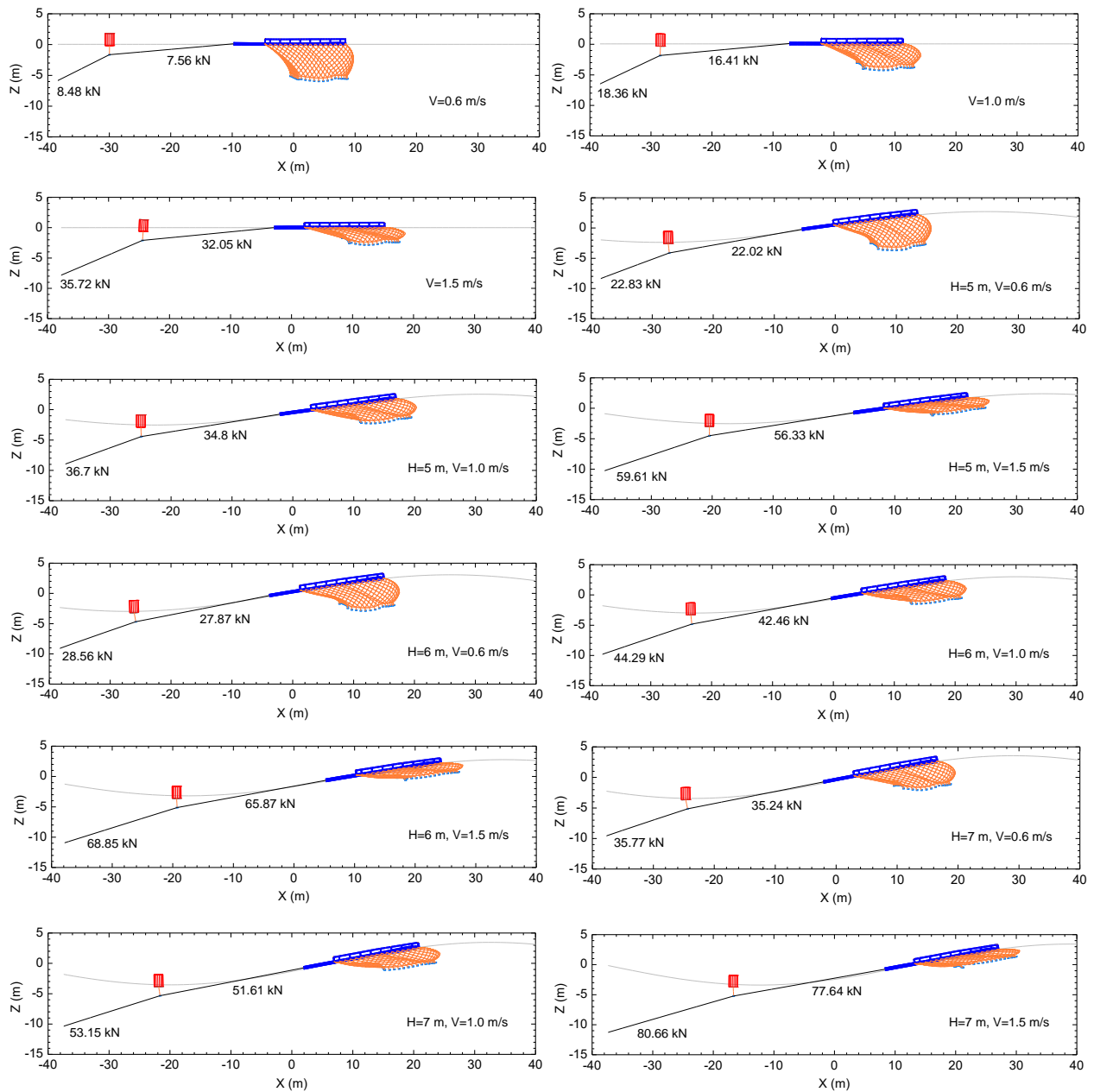


Figure 7. Deformation of the SPM cage system at the instant of maximum mooring line tension occurrence under waves combined with currents. The top line is the water surface.

Table 2. Deformation at different points on the floating collar

Point of the collar	Max bending moment (kN.m)	Max von Mises strain (%)	Max von Mises stress (MPa)
A (-11.78, 0.0, 0.0)	28.70	1.34	13.07
B (-6.58, 0.0, 0.0)	6.86	0.42	3.98
C (-6.58, 3.80, 0.0)	39.65	1.80	17.14
D (0.0, 7.60, 0.0)	54.09	2.39	22.79
E (5.89, 10.20, 0.0)	4.93	0.22	2.19
F (3.29, 5.70, 0.0)	2.24	0.17	1.61
G (6.58, 3.80, 0.0)	5.22	0.23	2.21
H (6.58, 0.0, 0.0)	21.37	0.92	8.78

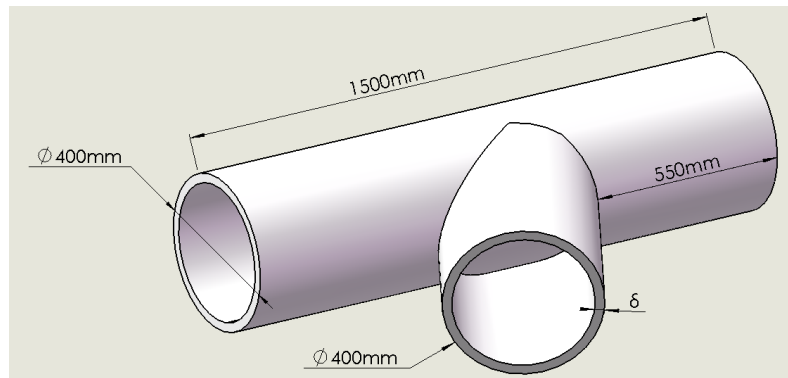


Figure 8. Component for connecting the floating pipes.

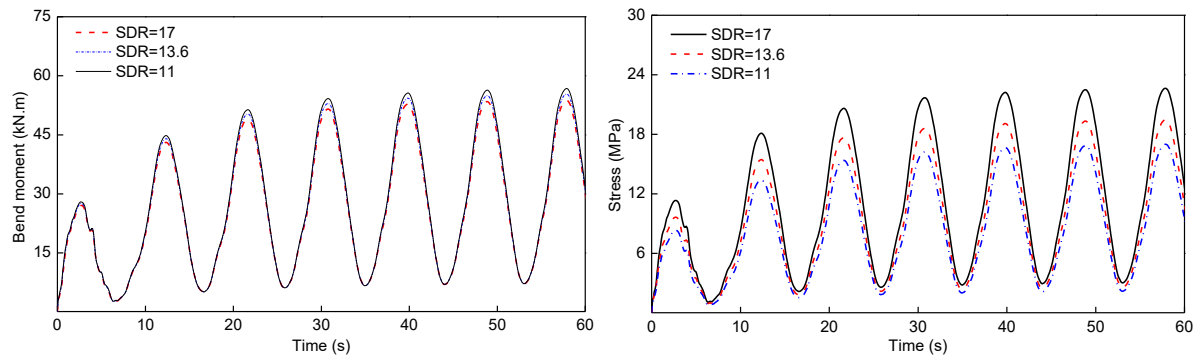


Figure 9. Bending moment and von Mises stress at point D attached to the connected component with various values for SDR.

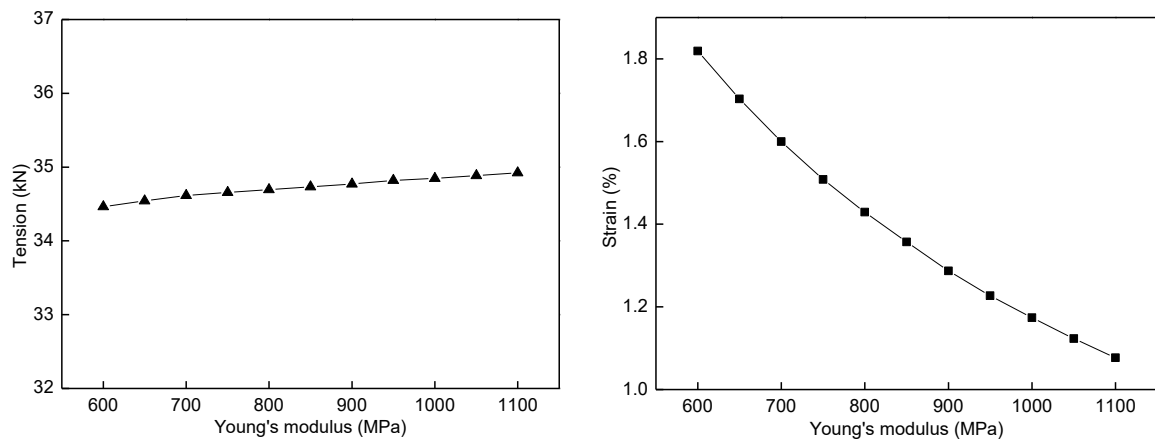


Figure 10. Mooring line tension and deformation of the floating collar with different values of Young's modulus.

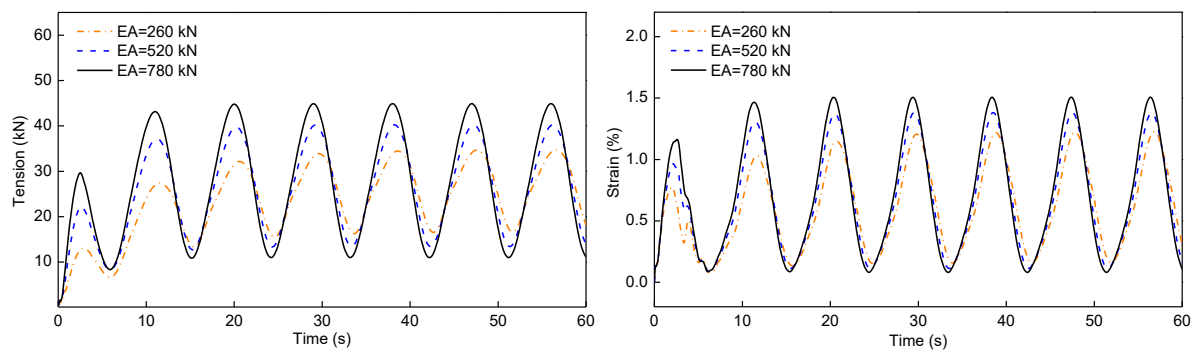


Figure 11. Mooring line tension and deformation of the floating collar with different axial stiffness values.

Conclusions

In this study, we developed a numerical model to simulate the dynamic response of an SPM cage system modeled as a combination of line elements and buoys with three and six degrees of freedom. Using the numerical model, we analyze the mooring line tension and deformation for the SPM cage collar under various wave-current conditions, where the effects of the mooring line arrangement, waves combined with a current, and material characteristicst are discussed in detail. According to our numerical results, we can make the following conclusions:

(1) Adding a buoy as a part of a cage system could reduce the force and deformation of the cage collar, where the current contributes greatly to the total load on the cage system when exposed to waves combined with a current.

(2) When the SPM cage is subjected to sea loads with waves (height = 7 m and period = 9 s) and a current velocity of 1.5 m/s, the maximum tension is 77.64 kN and the maximum stress on the collar is 22.79 MPa, which are the largest among all of the different wave-current conditions.

(3) Using a connected component with a lower SDR can effectively reduce the deformation of the floating pipes to avoid the plastic failure in the cage collar.

(4) The change in the mooring line tension is insignificant as Young's modulus increases for the floating pipes, but the deformation of the collar structure decreases sharply. In addition, a mooring system with higher stiffness can result in higher mooring line tension and greater deformation of the collar structure.

Acknowledgements

This study was supported by the National Natural Science Foundation of China (Nos. 31402349 and 31772897), Science and Technology Major Project of Hainan Province (No. ZDKJ2016011), Pearl River S&T Nova Program of Guangzhou (No. 201710010168), and Demonstration Project of Marine Economy Innovation and Development (No. Bhsfs012).

References

- Bessonneau, J.S., & Marichal, D. (1998). Study of the dynamics of submerged supple nets (applications to trawls). *Ocean Engineering*, 25(7): 563–583. [http://dx.doi.org/10.1016/S0029-8018\(97\)00035-8](http://dx.doi.org/10.1016/S0029-8018(97)00035-8).
- DeCew, J., Fredriksson, D.W., Lader, P.F., Chambers, M., Howell, W.H., Osenki, M., Celikkol, B., Frank, K., & Høy, E. (2013). Field measurements of cage deformation using acoustic sensors. *Aquacultural Engineering*, 57(6): 114–125. <http://dx.doi.org/10.1016/j.aquaeng.2013.09.006>
- DeCew, J., Tsukrov, I., Risso, A., Swift, M.R., & Celikkol, B. (2010). Modeling of dynamic behavior of a single-point

- moored submersible fish cage under currents. *Aquacultural Engineering*, 43(2): 38–45. <http://dx.doi.org/10.1016/j.aquaeng.2010.05.002>.
- Ding, D.L., Liu, W.H., & Ou, C.H. (2007). Use of non-linear regression to evaluate drag force and volume coefficient of structure of square cage. *Fisheries Science*, 73(6): 1249–1256. <http://dx.doi.org/10.1111/j.1444-2906.2007.01462.x>.
- FAO. (2016). The State of World Fisheries and Aquaculture. Retrieved from <http://www.fao.org>.
- Fredriksson, D.W., DeCew, J.C., & Tsukrov, I. (2007). Development of structural modeling techniques for evaluating HDPE plastic net pens used in marine aquaculture. *Ocean Engineering*, 34(16): 2124–2137. <http://dx.doi.org/10.1016/j.oceaneng.2007.04.007>.
- Goudey, C.A., Loverich, G., Kite-Powell, H., & Costa-Pierce, B. A. (2001). Mitigating the environmental effects of mariculture through single-point moorings (SPMs) and drifting cages. *Ices Journal of Marine Science*, 58 (2): 497–503. <http://dx.doi.org/10.1006/jmsc.2000.1033>
- Hao, S.H. (2008). The study of fluid-structure interaction of the flotation ring of a gravity-type fish cage (PhD Thesis). Dalian University of Technology, Dalian, China.
- Haritos, N., & He D.T. (1992) Modelling the response of cable elements in an ocean environment. *Finite Elements in Analysis & Design*, 11(1): 19–32. [http://dx.doi.org/10.1016/0168-874X\(92\)90026-9](http://dx.doi.org/10.1016/0168-874X(92)90026-9).
- Huang, C.C., Tang, H.J., & Liu, J.Y. (2008). Effects of waves and currents on gravity-type cages in the open sea. *Aquacultural Engineering*, 38(2): 105–116. <http://dx.doi.org/10.1016/j.aquaeng.2008.01.003>.
- Huang, X.H., Guo, G.X., Tao, Q.Y., Hu, Y., Liu, H.Y., Wang, S.M., & Hao, S. H. (2016). Numerical simulation of deformations and forces of a floating fish cage collar in waves. *Aquacultural Engineering*, 74: 111–119. <http://dx.doi.org/10.1016/j.aquaeng.2016.07.003>.
- Huang, X.H., Guo, G.X., Tao, Q.Y., Hu, Y., Liu, H.Y., Wang, S.M., & Hao, S. H. (2018). Dynamic deformation of the floating collar of a net cage under the combined effect of waves and current. *Aquacultural Engineering*, 83: 47–56. <http://dx.doi.org/10.1016/j.aquaeng.2018.08.002>.
- Klebert, P., Patursson, Ø., Endresen, P.C., Rundtop, P., Birkevold, J., & Rasmussen, H.W. (2015). Three-dimensional deformation of a large circular flexible sea cage in high currents: Field experiment and modeling. *Ocean Engineering*, 104: 511–520. <http://dx.doi.org/10.1016/j.oceaneng.2015.04.045>.
- Kristiansen, T., & Faltinsen, O.M. (2012). Modelling of current loads on aquaculture net cages. *Journal of Fluids and Structures*, 34(4): 218–235. <http://dx.doi.org/10.1016/j.jfluidstructs.2012.04.001>.
- Kristiansen, T., & Faltinsen, O.M. (2015). Experimental and numerical study of an aquaculture net cage with floater in waves and current. *Journal of Fluids and Structures*, 54: 1–26. <http://dx.doi.org/10.1016/j.jfluidstructs.2014.08.015>.
- Lader, P. F., & Enerhaug, B. (2005). Experimental investigation of forces and geometry of a net cage in uniform Flow. *IEEE Journal of Oceanic Engineering*, 30(1): 79–84. <http://dx.doi.org/10.1109/joe.2004.841390>
- Li, L., Fu, S.X., & Xu, Y.W. (2013). Nonlinear hydroelastic analysis of an aquaculture fish cage in irregular waves. *Marine Structures*, 34(34): 56–73. <http://dx.doi.org/10.1016/j.marstruc.2013.08.002>.

- Moe, H., Fredheima, A., & Hopperstad, O. S. (2010). Structural analysis of aquaculture net cages in current. *Journal of Fluids and Structures*, 26(3): 503–516. <http://dx.doi.org/10.1016/j.jfluidstructs.2010.01.007>.
- Orcina Ltd. (2015). OrcaFlex Manual version 10.0a. Retrieved from <http://www.orcina.com>.
- Shainee, M., DeCew, J., Leira, B. J., Ellingsen, H., & Fredheim, A. (2013). Numerical simulation of a self-submersible SPM cage system in regular waves with following currents. *Aquacultural Engineering*, 54(3): 29–37. <http://dx.doi.org/10.1016/j.aquaeng.2012.10.007>.
- Stranda, I.M., Sørensen, A.J., Volentb, Z., & Lader, P. (2016). Experimental study of current forces and deformations on a half ellipsoidal closed flexible fish cage. *Journal of Fluids and Structures*, 65: 108–120. <http://dx.doi.org/10.1016/j.jfluidstructs.2016.05.011>.
- Xu, T. J., Dong, G. H., Li, Y. C., & Wei, W. J. (2014). Numerical study of a self-submersible single-point mooring gravity cage in combined wave-current flow. *Applied Ocean Research*, 48: 66–79. <http://dx.doi.org/10.1016/j.apor.2014.07.014>.
- Xu, T. J., Zhao, Y. P., Dong, G. H., & Gui, F. K. (2013). Analysis of hydrodynamic behavior of a submersible net cage and mooring system in waves and current. *Applied Ocean Research*, 42(3): 155–167. <http://dx.doi.org/10.1016/j.apor.2013.05.007>.
- Xu, T.J., Hou, H.M., Dong, G.H., Zhao, Y.P., & Guo, W.J. (2017). Structural analysis of float collar for metal fish cage in waves. *Turkish Journal of Fisheries and Aquatic Sciences*, 17: 257-268. http://dx.doi.org/10.4194/1303-2712-v17_2_04.